Title: Calcium: Modulator of Post-transcriptional and post-translational process in mESCs

Shikha Sharma[1,2], Dasaradhi Palakodeti[1], Tina Mukherjee[1]

Author List

Dr Shikha Sharma[1]: First author, lead contact and corresponding author

Dr Dasaradhi Palakodeti[1]

Dr Tina Mukherjee[1]

Affiliations:

1) Institute for Stem Cell Science and Regenerative Medicine (inStem), Bangalore, India
2) Lead contact and corresponding author: shikha.ss19254@gmail.com

Abstract

Calcium ion (Ca^{2+}) is a ubiquitous intracellular and extracellular messenger that regulates several cellular activities. Previous findings have reported the presence of active Ca^{2+} receptors in mouse embryonic stem cells (mESCs) but the fundamental requirement of Ca^{2+} signalling remains unclear. We have noted the presence of high Ca^{2+} in undifferentiated mESCs and showed that its depletion exerts G2/M cell cycle arrest, spontaneous differentiation of mESCs towards mesoderm lineage and mitochondrial biogenesis. Further, our data demonstrates that Ca^{2+} regulates the homeostasis and stability of Oct4 and Nanog at the post-translational level through pCamkIIα dependent mechanism independent of polyubiquitin system, JAK-STAT3 pathway, transcriptional and translational control. Our data also signifies the role of Ca^{2+} at the post-transcriptional level in regulating p-bodies and stress granule markers (Dcp1a, XRN1, Tudor and EDC4), splicing-dependent and 3'UTR-dependent NMD activity. Together, this study identifies the broad role of Ca^{2+} in modulating key processes in mESCs.

Keywords: Calcium; p-bodies; cell-cycle arrest; NMD; mitochondrial biogenesis

Highlights

- Ca^{2+} is present at elevated levels in mESCs and is important for pluripotency
- Ca^{2+} depletion accelerates G2/M cell cycle arrest and mesoderm differentiation
- Ca^{2+} regulates pluripotency and p-bodies markers at the post-translational level
- Ca^{2+} regulates Oct4, Nanog, dcp1a through pCamkIIα dependent mechanism

Affiliations:

1) Institute for Stem Cell Science and Regenerative Medicine (inStem), Bangalore, India
2) Lead contact and corresponding author: shikha.ss19254@gmail.com

Introduction

Embryonic stem cells (ESCs) are derived from the inner cell mass (ICM) of embryos defined by eminent features such as pluripotency, self-renewal and limitless proliferation (Ye et al., 2024). Several studies have shown that the ESCs core pluripotency network is regulated by diverse molecular mechanisms, extracellular signalling pathway, post-transcriptional regulation, epigenetic mechanism, and chromatin remodelling (Yeo and Ng 2013, Kobayashi et al., 2015). The ability of ESCs to differentiate into all three lineages of an organism makes them an ideal candidate for basic research on pluripotency, genomic engineering, cell identity transition, disease modelling, cell therapy and regenerative medicine (Czechanski et al., 2014, Kobayashi et al., 2015). Further understanding the regulation of ESCs pluripotency network will provide more insight into the nature of pluripotent stem cells.

Ca^{2} is a fundamental regulator of several processes such as cell cycle, cell proliferation, neuronal plasticity, gene regulation and apoptosis (Clapham DE 2007, Berridge et al., 2003). Despite the broad role of Ca^{2+}signalling in different cell types, there are only a few studies that have reported the presence of Ca^{2+} signalling in pluripotent stem cells. In 2004, Yanagida et al., documented the activation of various Ca^{2+} receptors upon stimulation in mESCs indicating the presence of calcium-regulating pathways. Todorova et al., (2009) observed the activation of Ca^{2+} signalling by lysophosphatidic acid (LPA) in mESCs. In 2010, Schwirtlich et al. reported that GABA-mediated Ca^{2+} signalling is important for the proliferation and differentiation of mESCs. However, the role of Ca^{2+}signalling in the regulation of pluripotency remains unclear. In this study, we have reported the role of Ca^{2+} signalling in regulating proliferation, cell cycle, p-bodies dynamic and core pluripotency markers of

1) Institute for Stem Cell Science and Regenerative Medicine (inStem), Bangalore, India
2) Lead contact and corresponding author: shikha.ss19254@gmail.com

mESCs. Our data indicates that high Ca^{2+} is important for the maintenance of pluripotency in mESCs at the post-transcriptional and post-translational levels.

Results

Pluripotent stem cells maintain an elevated level of cytosolic calcium

It is not yet clear why ESCs maintain a high level of Ca^{2+} within their cytoplasm. Therefore, we became interested to understand the role of Ca^{2+} in mESCs. We manipulated the level of Ca^{2+} in the presence of LIF using BAPTA and thapsigargin. BAPTA is a cell-permeable Ca^{2+}chelator and thapsigargin is a SERCA pump inhibitor (Collatz et al., 1997, Lytton et al., 1991). We observed using Fluo-4 staining that supplementation of BAPTA 2uM (B2uM) for 72hrs was able to reduce the level of Ca^{2+} in mESCs comparable to without LIF condition while thapsigargin 1nM (T1nM) treatment increased the calcium level (Figure 1A and D). We also noted that Ca^{2+} was downregulated in the without LIF condition (C-L) and supplementation of T1nM was able to increase the Ca2+ level slightly but unable to bring it back to the control condition (C+L) (Figure 1A and 1D). We also detected heterogeneity in the level of Ca^{2+} in cells within mESCs colonies (Figure 1A). In addition, we noted that B1uM also reduced the Ca^{2+} level in the different organelles such as endoplasmic reticulum (ER) (Figure 1B and 1E) and lysosomes (Figure 1C) of mESCs. Conversely, T1nM increased the overall Ca^{2+} level in the lysosomes (Figure 1C) but not in the ER (Figures 1B and 1E).

Further, we have observed a decrease in the proliferation of mESCs with the increase in the concentration of bapta (B1uM, B2uM, and B5uM) in 72 hrs (Figure 1F). We noted that mESCs colonies exhibited fibroblast morphology upon differentiation and observed increased differentiation with increasing concentrations of bapta (B1uM and B2uM) (S1_Figure S2C

Affiliations:

1) Institute for Stem Cell Science and Regenerative Medicine (inStem), Bangalore, India
2) Lead contact and corresponding author: shikha.ss19254@gmail.com

and 2D). Indeed, we also observed that differentiation was less in bapta-treated samples as compared to C-L but they exhibited fibroblast morphology similar to C-L condition (supp file (S1)_Figure S2C and 2D). We further replaced B2uM media after 72hrs with control ESC media (B2R) for 48hrs and observed an increase in the proliferation of mESCs indicating bapta treatment is reversible (Figure 1G). However, we noted that mESCs which underwent complete morphological change (fibroblast appearance) were unable to proliferate further and retained their phenotype. We next checked the level of cMyc within these mESCs and observed that cMyc expression goes down upon B2uM treatment in 72 hrs independent of transcriptional control (Figure 1H and 1K). We further observed an increase in the expression of cMyc in B2R as compared to B2uM in 5 days (Figure 1I and 1J). Besides this, we analysed the cell cycle profile of C+L, B2uM, and B2R mESCs in 72 hrs (Figure 1L) and 5 days (Figure M) and observed that bapta treatment resulted in the cell cycle arrest at G2/M which was reversible with B2R treatment (Figure M). Further, we also noted that B2uM and C-L resulted in the fluctuation in the expression of calcium receptors of the plasma membrane, ER and mitochondria including SERCA PMCA, IP3, STIM, ORAI, Ryanodine, and MCU (S1_Figure S 1C, D, E, F, G, H) signifies that bapta treatment might be affecting the level of Ca^{2+} within different organelles.

Calcium homeostasis is critical for pluripotency

To explore the role of Ca^{2+} in the maintenance of pluripotency in mESCs, We checked the expression of pluripotency markers upon bapta and thapsigargin treatment. Western blot and immunofluorescence (IF) data confirmed the increase/decrease in the protein level of core pluripotency markers including Oct4 and Nanog upon low/high Ca^{2+} condition using bapta (B1uM and B2uM) and thapsigargin 250 pm, 500pm and 1nM (T250pm, T500pm, T1nM) in

Affiliations:

1) Institute for Stem Cell Science and Regenerative Medicine (inStem), Bangalore, India
2) Lead contact and corresponding author: shikha.ss19254@gmail.com

the presence of LIF suggesting that Ca^{2+} has role in the regulation of pluripotency markers (Figure 2 A, B, E, F and M). Moreover, we noted the heterogeneity in the expression of Oct4 and Nanog in cells within mESCs colonies (Figure 2A and 2B) which also corroborates with the heterogeneous level of Ca^{2+} in cells within mESCs (Figure 1A). Next, we have not observed any significant difference in the expression Oct4, Nanog and cMyc in the absence of LIF and the presence of thapsigargin (Figure 2 A, B, G, H and M). CHIR 99021 (CH) and PD0325901 (PD) are inhibitors of glycogen synthase kinase 3 beta (GSK3β) and MAPK/ERK signalling pathways, also known as 2i inhibitors implicated for the maintenance of the ground state of mESCs (Sim et al., 2017). Furthermore, we subjected mESCs to 2i inhibitor treatment in the presence of LIF and B1uM and observed a decrease in the expression of Oct4 and Nanog in the presence of B1uM, LIF and 2i inhibitor (Figure S2A) which signifies that Ca^{2+} regulates the expression of pluripotency markers under naive and ground state of mESCs. We also discerned that some of the mESCs colonies exhibited fibroblast morphology upon B1uM treatment in the presence of a 2i inhibitor (S1_Figure S2B).

pCamkIIα is a downstream target of Ca^{2+} signalling. Our data showed Ca^{2+}-dependent simultaneous upregulation/downregulation of pCamkIIα and Oct4 in mESCs upon B2uM and T1nM treatment (Figure 2B, 2C, and 2M). We further noted that pCamkIIa is present mainly in the nucleus of mESCs and observed the co-localization of pCamkIIα with Oct4 (Figure 2E, yellow) indicating that Ca^{2+} might have a role in the regulation of phosphorylation of pluripotency markers through pCamkIIα dependent mechanism. Previous reports suggest that LIF plays a major role in maintaining the pluripotency of mESCs mainly through the JAK-STAT3 pathway (Tang et al., 2013). We asked if Ca^{2+} regulates the LIF signalling by

Affiliations:

1) Institute for Stem Cell Science and Regenerative Medicine (inStem), Bangalore, India
2) Lead contact and corresponding author: shikha.ss19254@gmail.com

controlling the JAK-STAT pathway in mESCs. We observed that the protein level of pSTAT3 was unchanged upon B1uM, B2uM, T250pM, T500pM, and T1nM treatment in the presence and absence of LIF suggesting that Ca^{2+} act independent of the JAK-STAT3 pathway for the maintenance of pluripotency of mESCs (Figure 2 E, F, and H). Further, we checked the transcript level of Oct4, Nanog, Sox2 and Klf4, and early differentiation markers of mesoderm (Mixl1, Brachyury), endoderm (Sox17, and MeoX1), and ectoderm (Sox1, and Pax6) upon Ca^{2+} manipulation using B2uM and T1nM and observed no change in the transcript level of these markers in 48hrs (S2 Figure S1 A and B) and 4 days (Figure 2I and J). Therefore, our data indicate that Ca^{2+} might be playing a role in the regulation of pluripotency and differentiation markers at the post-transcriptional, translational and post-translational levels.

Besides this, we observed an increase in the cytoplasm-to-nucleus ratio of mESCs by decreasing the level of Ca^{2+} using B2uM and C-L condition and a decrease in cytoplasm-to-nucleus ratio upon T1nM treatment by phalloidin staining shown by arrow (Figure 2K and 2L). Park et al., have also demonstrated that high cytosolic Ca^{2+} results in a decreased cytoplasm/nuclear ratio in drosophila C4da neurons (Park et al.,2020) which also corroborates with our findings and indicates the possible role of Ca^{2+} in cytoskeleton remodelling for cell shape transition. Cadherin-adhesion complex is important for bridging cell-to-cell contact and drives various morphogenetic changes (Mege et al., 2017). Therefore, we checked the expression of calcium-dependent adhesion protein E-cadherin and found its expression downregulated in mESCs upon B2uM treatment and increased upon T1nM condition indicating the involvement of Ca^{2+}-dependent cadherin family proteins for driving morphological changes in ESCs upon Ca^{2+} manipulation (Figure 2N).

Affiliations:

1) Institute for Stem Cell Science and Regenerative Medicine (inStem), Bangalore, India
2) Lead contact and corresponding author: shikha.ss19254@gmail.com

Calcium is important for the regulation of ribonucleoprotein complexes and NMD activity

To understand whether Ca^{2+} has any role at the post-transcriptional level. We examined the expression of p-bodies and stress granule markers upon Ca^{2+} manipulation in mESCs. Our data showed that dcp1a, xrn1, Tudor and β-actin are present abundantly in both cytoplasm and nucleus of undifferentiated mESCs (Figure 3A and 3B, S1_Figure S3 A, B, C, and D) and observed a decrease/increase in the expression of these mRNP granules upon B2uM and T1nM treatment (Figure 3A, B, D; Figure S3 A, B, C, D, E). We also noted the variation in the size of these granules as some were large in size and others small (Figure 3B). The variations in size could be due to several reasons such as a) These markers may be a part of several complexes having different compositions either present as a monomer or dimer b) they may be at different stages of maturation for post-transcriptional processes to carry out their functions. Further, we have observed the co-localization of dcp1a with β-actin, xrn1, tudor and pCamkIIα indicating that Ca^{2+} might be regulating p-body markers through pCamkIIα dependent mechanism (Figure 3B). However, we were unable to check the co-localization of other markers as both the antibodies were raised in the same species. Our data also shows that Ca^{2+} regulate p-bodies and stress granule markers independent of transcriptional control (Figure 3C). Next, we have quantified splicing-dependent nonsense-mediated mRNA decay (NMD) activity and long 3' UTR-dependent NMD activity using two fluorescent reporter proteins green TagGFP2 and far-red Katushka as described by Pereverzev et al. 2015 in the presence of B2uM and C-L condition. We have observed increased splicing-dependent NMD activity (Figure 3E and 3F) and decreased 3' UTR NMD

Affiliations:

1) Institute for Stem Cell Science and Regenerative Medicine (inStem), Bangalore, India
2) Lead contact and corresponding author: shikha.ss19254@gmail.com

activity (Figure 3G and 3H) in mESCS treated with B2uM and C-L conditions suggesting that Ca^{2+} exerts the opposite effect on splicing dependent and 3'UTR dependent NMD pathway in mESCs.

Calcium doesn't control the expression of pluripotency and differentiation markers at post-transcriptional and translational level

We checked the global translation rate through polysome profiling and observed no change in the global translational rate upon Ca^{2+} manipulation with B2uM (Figure 4A). However, we observed that the expression of early translation initiation marker elf1a was downregulated in B2uM-treated mESCs (Figure 4B). which indicates a possibility of differential expression of translation markers upon Ca^{2+} manipulation. As we have observed no change in the transcription of pluripotency and differentiation markers in control and B2uM-treated mESCs. We sought to find whether Ca^{2+} suppress the translation of pluripotency/differentiation markers by holding them in p-bodies/stress granules. To address this, we performed polysome profiling of mESCs treated with B2uM and collected cytoplasmic fraction (composed of mRNP granules), 80s ribosomal subunit (80s), and polysome fraction and checked the expression of Oct4, Nanog, Sox2, and Klf4 and early differentiation markers of mesoderm, and ectoderm such as Mixl1, Brachyury, Pax6 exhibiting high CT value. We were unable to detect any significant difference in the transcript level of both pluripotency and differentiation markers in the cytoplasmic fraction of mRNP granules, the 80S and polysome fraction of control and B2uM treated samples (Figure 4D and 4E) indicating that pluripotency and differentiation markers are not held by p-bodies. To address this further, we blocked the transcription and translation of control, B1uM, T1nM and C-L treated mESCs after 72hrs with combined actinomycin D (ACD) cycloheximide

Affiliations:

1) Institute for Stem Cell Science and Regenerative Medicine (inStem), Bangalore, India
2) Lead contact and corresponding author: shikha.ss19254@gmail.com

(CHX) treatment for 2hr and checked the expression of pluripotency and mesodermal differentiation markers and observed no significant change in their expression which illustrate that Ca^{2+} doesn't regulate core pluripotency and differentiation markers at post-transcriptional level (Figure 4F and 4G).

It is well known that undifferentiated ESCs do not express differentiation markers. We noted that the transcript level of early differentiation markers such as MixL1 and Brachyury were expressed at CT values of 28±1 and 28±1 respectively while MeoX1 expressed a CT value of 28±1 and SOX17 was mostly undetermined or expressed at CT value 34±1, Pax6 and SOX1 were present at CT value 26±1 and 26±1 respectively in undifferentiated mESCs. These CT values signify that transcript of differentiation markers are present at a low level in undifferentiated mESCs. In addition, we detected transcript of differentiation markers (MixL1, Brachyury and Pax6) in a polysome fraction of control and B2uM treated mESCs which indicates that differentiation markers are undergoing translation and might be expressed in undifferentiated mESCs or getting degraded. Since these mESCs showed the tendency to spontaneous differentiation towards mesoderm lineage. We have checked the expression of only brachyury protein in control, B2uM and C-L condition (Figure 4H). We have observed some background expression of brachyury in undifferentiated mESCs and its increased expression in B2uM and C-L conditions (Figure 4H) which indicates the role of calcium in the degradation of brachyury protein. Next, we also performed mitotracker-red staining and noted the increase in the size and number of mitochondria upon calcium reduction with B2uM and C-L condition in 48hrs (figure 4 I, and 4J), We observed globular mitochondria in control mESCs and a network of branched mitochondria in B2uM and C-L in

Affiliations:

1) Institute for Stem Cell Science and Regenerative Medicine (inStem), Bangalore, India
2) Lead contact and corresponding author: shikha.ss19254@gmail.com

48hrs (Figure 4I) indicating mitochondria undergo a morphological change from globular to tubular form upon Ca^{2+} reduction.

Calcium is important for the stability of pluripotency markers, p-body and stress granule markers and degradation of differentiation markers

Further, we asked whether Ca^{2+} plays a role in the degradation of proliferation, differentiation, core pluripotency markers, polyubiquitin marker (pUBQ), p-body and stress granule markers at posttranslational level. Our data demonstrate an increase in the expression of cMyc, dcp1a, tudor, Oct4, and pUBQ in both control and B2uM treated mESCs upon MG132 treatment (Figure 5 A, B, C, D, E, F, G) which suggests that Ca^{2+} level might be important for the maintenance of homeostasis and stability of these proteins. Further, we also observed increased expression of brachyury in control condition after MG2132 treatment which also corroborates with the increased expression of brachyury upon B2uM treatment but MG132 was unable to increase the brachyury protein expression in B2uM treated mESCs but rather it led to its decreased expression (Figure 5A, D). Earlier findings have suggested that proteasomal inhibition can lead to the degradation of proteins through the activation of other degradation pathways such as autophagy (Wang et al., 2019). Furthermore, we noted that MG132 treatment was able to rescue only partial protein level of dcp1a and tudor in B2uM treated mESCs as compared to control mESCs (Figure 5B and 5F) which also implies the role of other signalling pathways in the regulation of p-body and stress granule markers upon Ca^{2+} reduction. Interestingly, we also noted the decrease in the expression of pUBQ upon B2uM treatment and its upregulation with MG132 treatment (Figure 5C, 5D) which suggests that Ca^{2+} regulate the stability of pluripotency markers independent of PUBQ proteasomal system upon Ca^{2+} reduction. Next, we observed a very low expression of LC3 in the undifferentiated

Affiliations:

1) Institute for Stem Cell Science and Regenerative Medicine (inStem), Bangalore, India
2) Lead contact and corresponding author: shikha.ss19254@gmail.com

mESCs which further decreased upon B2uM and C-L condition suggesting autophagy might not be playing a role in the degradation of pluripotency and differentiation markers upon Ca^{2+} reduction (Figure 5H). This also indicates that pUBQ proteasomal system might be important for the degradation of differentiation markers in undifferentiated mESCs and its low expression upon Ca^{2+} reduction is important for the stability of brachyury protein and activation of other signalling pathways apart from autophagy to determine lineage specificity. We have further checked the stability of Oct4 and Nanog using a CHX chase assay as described by Kao et al., 2015. We chased the expression of Oct4 and Nanog for 1hr 20 min with a 20 min time interval and observed that their degradation was faster in B2uM-treated mESCs indicating that Ca^{2+} is important for the maintenance of the stability of core pluripotency markers (Figure 5I). Furthermore, we observed an increase in the level of Oct4 and Nanog proteins in B2uM-treated mESCs through western blot (Figure 5 J) suggesting that Ca^{2+} maintains the stability of pluripotency markers at the post-translational level.

Calcium maintains the stability of OCT4, NANOG and DCP1a by pCAMKII alpha-dependent mechanism

We further asked whether Ca^{2+} maintains the pluripotency of mESCs through the pCamkIIα dependent mechanism. We used the electroporation method to deliver the pCamkIIα shRNA to silence its expression. We noted that 80-90% of mESCs expressed pCamkIIα shRNA as shown by their GFP expression (Figure 6A). Moreover, we observed that pCamkIIα shRNA (pCamkIIα KD) treated mESCs exhibited fibroblast-like morphology (Figure 6B and C) which was similar to the phenotype shown by B2uM treated mESCs (Figure 2K). However, we were unable to detect any significant decrease in the level of pCamkIIα mRNA but observed a decrease in the level of pCamkIIα protein upon pCamkIIα KD (Figure 6D and 6I)

Affiliations:

1) Institute for Stem Cell Science and Regenerative Medicine (inStem), Bangalore, India
2) Lead contact and corresponding author: shikha.ss19254@gmail.com

which suggests a possibility that pCamkIIα shRNA might have exerted different mechanism in regulating pCamkIIα expression may be through stress granules or translational control. Furthermore, we detected a significant decrease in the expression of Oct4 and Nanog proteins upon pCamkIIα KD by western blotting (Figure 6F), however, we did not observe any change in the transcript level of both pluripotency and differentiation marker (Figure 6M and 6N) similar to B2uM treated mESCs (Figure 2I, J). In addition, we observed that the pSTAT3 protein level was unaffected in pCamkIIα KD mESCs which again signifies that Ca^{2+} acts independently of the JAK-STAT pathway (Figure 6F). We further observed a decrease in the expression of p-body marker dcp1a upon pCamkIIα KD (Figure 6I) which indicates that Ca^{2+} is important for the stability of dcp1a through pCamkIIα dependent mechanism. Furthermore, we also performed SERCA R2 receptor knockdown (SER R2 KD) by using shRNA against its highly expressed receptor2 which we have noted in our QPCR data. We observed a decrease in the mRNA pool of the SERCA R2 receptor upon SER R2 KD (Figure 6D). We noted that SER R2 KD mESCs exhibited compact colonies as compared to control mESCs (Figure 6B and C) which was similar to T1nM-treated mESCs (Figure 2K). Further, we observed an increase in the expression of Oct4 and Nanog proteins upon SER R2 KD (Figure 6 G) which signifies that cytoplasmic Ca^{2+} is important for their stability. We observed no change in the transcript level of pluripotency and differentiation marker (Figures 6M and 6N) as well as in the protein level of pSTAT3 in SER R2 KD mESCs (Figure 6G) again signifying that calcium acts independently of the JAK-STAT pathway. Furthermore, we also observed an increase in the expression of dcp1a and pCamkIIα upon serca R2 KD (Figure 6H) which symbolizes that cytosolic Ca^{2+} plays a role in the biogenesis of dcp1a through pCamkIIα.

Affiliations:

1) Institute for Stem Cell Science and Regenerative Medicine (inStem), Bangalore, India
2) Lead contact and corresponding author: shikha.ss19254@gmail.com

Identification of phosphoproteins altered upon calcium manipulation using phosphoproteomics approach

We compared the phosphoproteomics profile of control and B2uM-treated mESCs. We identified 53 phosphoproteins (PP) that were significantly upregulated and 35 PP downregulated in B2uM samples (n=2) shown by the heat map (Figure 7A). Using Proteome Discoverer Software (Thermo Fisher Scientific), we detected the phosphosites in the identified phosphopeptides from mass spectrometry (MS) data and observed majorly serine-threonine phosphosites along with a few tyrosine sites (supp excel sheet S2). Further using ShinyGO 0.80 software we carried out the KEGG pathway, tree plot, GO cellular component (GOC), and string function enrichment analysis for the differentially expressed phospho-proteins (DEPP) represented in the heat map (Figure 7B, C, D, E, F). We observed that spliceosome and mRNA surveillance PP were highly enriched in our dataset and carried out further KEGG pathway enrichment analysis for them (Figure 7G, H) and observed our PP are part of these complexes labelled as red. We further observed that DEPP exhibits 1385 protein-protein interactions (PPI) with an expected 689 PPI (p=0) using string PPI network analysis (Figure 7I). Next, we identified DEPP related to different pathways using string bio process enrichment analysis (SBPEA). As we have observed change in mitochondrial biogenesis, we conducted GO biological function (GOB), GO molecular function (GOF) and GOC analysis for DEPP related to metabolism listed in S4 A legend and observed that they are the positive and negative regulator of metabolism, part of mRNP complex and displayed nuclear and organelle localization which suggests a widespread functional role of these proteins (S1_Figure S4A, B, C). Further, we carried out the GOC analysis of a few DEPP including Hk2, Hspa8, Atp5a1, Cox4i1, Pkm, and Gapdh identified for ATP metabolism and observed they have mitochondrial localization (S1_Figure S4J) which signifies their role in

Affiliations:

1) Institute for Stem Cell Science and Regenerative Medicine (inStem), Bangalore, India
2) Lead contact and corresponding author: shikha.ss19254@gmail.com

mitochondrial biogenesis and oxidative phosphorylation. We also noted that several PP related to translational machinery including Rps18, Rp16, Eif3c, Abcf1, Eef1a1, Eef2, Eif5a, Rpl18a, Eif2s1, Rpl5, Rplp2, Rpl34, Eef1d, Rpl27, Eif3b, Rpl23a, Rps8, and Larp1 were highly differentially regulated despite global translation rate was unaffected upon Ca^{2+} reduction and conducted GOC, GOB network and GOF analysis for them (S1_Figure S4 G, H I). We observed that these proteins are also part of mRNP complex and has role in macromolecule biosynthetic pathway which exemplify their other role apart from controlling translation rate. Next, we further performed the GOB and GOF analysis for DEPP implicated in nucleosome and chromatin assembly including Smarcd1, Nasp, Hat1, Atrx, and Nap1l1 (S1_Figure S4 D, E) and observed they have chromatin and histone binding properties and has a role in DNA replication-independent chromatin assembly. Further we conducted GOB network analysis of DEPP including CSe1, smarcd1, Hk2, Pkm, Tfpt, Tcof1, champ1, nasp, Macf1, Hat1, Bcam, Atrx, Nmd3, Sde2, Ubr4, Hsph1, Trap1, nucks, Cdk1, Mki67, Tpx2, champ1 (S1_Figure S4 F) and observed they exhibit cross-talk in kinetochore process, chromatin condensation, nuclear division, mitotic cell cycle and chromatin remodelling. We have also detected some DEPP including Cdk1, Mki67, Nucks1, and Tpx2 crucial for mitotic cell division and mitochondrial ATP synthesis through GOB network analysis implicating their role in G2/M cell cycle arrest and oxidative phosphorylation (S1_Figure S5 A, B).

Discussion

In recent years, pluripotent stem cells have received extensive importance in the field of regenerative medicine to study cell development and differentiation. However, the role of Ca^{2+} signalling in the maintenance of pluripotency is not yet explored. Our previous work in drosophila has demonstrated that blood progenitors undergo differentiation upon Ca^{2+}

Affiliations:

1) Institute for Stem Cell Science and Regenerative Medicine (inStem), Bangalore, India
2) Lead contact and corresponding author: shikha.ss19254@gmail.com

reduction (Shim and Mukherjee et al., 2013). Our data showed that low calcium leads to the spontaneous differentiation of mESCs reflecting the broadly conserved phenomenon in stem/progenitor cells across the species. In stem cell biology, there is a persistent effort to understand the mechanism underlying ESC pluripotency. Nevertheless, the comprehensive repertoire of molecules involved in controlling the ESC state is not yet completely understood. Several studies have reported the heterogenous expression of Nanog in mESCs but the mechanism underlying the same is still unclear (Torres-Padilla and Chambers 2014). Our data indicates a correlation between the heterogenous expression of Oct4 and Nanog with the heterogenous level of Ca^{2+} in mESCs. Earlier findings suggest that the loss of Oct4 and Nanog expression in ESCs is associated with the differentiation of ESCs towards the endoderm lineage (Niwa et al., 2000, Hamazaki et al., 2004)). Interestingly, we noted that upon Ca^{2+} reduction mESCs showed the tendency to differentiate towards mesoderm lineage along with Oct4 and Nanog downregulation despite transcript of other lineages were also present in undifferentiated mESCs suggesting that Ca^{2+} signalling might be important in undifferentiated mESCs to mask the expression of mesoderm markers. Furthermore, our data signifies the role of high Ca^{2+} in mediating the degradation of brachyury protein and low calcium and low pUBQ proteasomal system for its stability which also suggests the activation of other signalling pathways upon calcium reduction to determine lineage specificity. Moreover, our data demonstrate that calcium acts independently of the LIF-JAK-STAT3 pathway for the regulation of core pluripotency and differentiation markers and has no role at the transcriptional level but controls the stability of these fundamental regulators at the post-translational level. Our pCamkIIα KD data indicate that pCamkIIα is important for the stability of Oct4 and Nanog protein in mESCs. We have also observed the co-localization of Oct4 and pCamkIIα. It is well known that pCamkIIα is a serine-threonine kinase and is

Affiliations:

1) Institute for Stem Cell Science and Regenerative Medicine (inStem), Bangalore, India
2) Lead contact and corresponding author: shikha.ss19254@gmail.com

involved in the phosphorylation of a wide array of proteins (Clapham 2007) thus suggesting that it might have a role in regulating the phosphorylation status of these core pluripotency markers. Earlier studies have demonstrated that phosphorylation of Oct4 and Nanog proteins at serine residue decreases their stability and dispenses them towards the pUBQ-mediated proteasomal degradation pathway in mESCs (Bae et al., 2017, Kim et al 2014). Our data demonstrate that Ca^{2+} regulates the stability of Oct4 and Nanog protein independent of the pUBQ system. Several reports suggest that protein degradation can happen independent of polyubiquitin tagging or without 19S proteasome subunit by 20S or 26S mediated proteolysis through structural disorder (Shang and Taylor 2011, Ben-Nissan and Sharon 2014). Previous findings have advocated that Ca^{2+} and Ca^{2+} binding proteins promote conformational change upon binding to target proteins and modulate their activity and stability (Strynadka and James, 1991, Clapham 2007, Hołubowicz et al., 2017). Therefore further structural, biochemical and molecular studies are needed to understand the in-depth mechanism of how Ca^{2+} regulate the activity and stability of pluripotency markers either through phosphorylation at specific residues or conformational change.

Interestingly, our data also signifies that Ca^{2+} has a role in controlling the expression of p-bodies and stress granule markers but has no role in controlling the expression of pluripotency and differentiation markers at a post-transcriptional level which indicates that Ca^{2+} might be regulating other signalling pathways at post-transcriptional level important for the maintenance of pluripotency of mESCs. Our data demonstrate that 3'UTR mediated NMD is important for the maintenance of pluripotency while splicing dependent NMD mechanism is more active during the differentiation process which signifies that Ca^{2+} plays a role in the modulation of different post-transcriptional processes. Our data has identified

Affiliations:

1) Institute for Stem Cell Science and Regenerative Medicine (inStem), Bangalore, India
2) Lead contact and corresponding author: shikha.ss19254@gmail.com

several RNA-binding and ribosomal PP including edc4, dcp1a, xrn1, tudor, Pa2g4, Nmd3, Ddx21, Srsf5, Srsf6, Srsf1, EDC4, Fkbp4, Cpsf3, Fip1l1, Hnrnpab, Hnrnpa, Hnrnpa3, Rbm39, Dhx15, Acin1, Snw1, Larp, Srrm1, Clasrp, Rps18, Rars, Eif3c, Eef1a1, Eif5a, Rpl18a, Eif2s1, Rpl5, Rps8, Rplp2, Rpl34, Eef1d, Rpl27, Eif3b, Rpl23a implicated in mRNP complex formation, alternative splicing, alternative polyadenylation, mRNA stability, 5′TOP mRNAs stability, miRNA biogenesis, mRNA decapping and NMD (Martinez et al., 2013, Hochstoeger et al., 2024, Chiang et al., 2013, Decker et al., 2012) which suggests a widespread role of Ca^{2+} at a post-transcriptional level rather than global translational control. Our data has revealed decreased expression of dcp1a, tudor and xrn1 and increased expression of edc4 upon Ca^{2+} reduction which signifies differential expression of p-bodies markers upon Ca^{2+} manipulation. Moreover, our data indicate that pCamkIIα is also a part of p-bodies component machinery which suggests that Ca^{2+} might be regulating the dynamic, composition, interaction and activity of p-bodies markers through regulating their phosphorylation status. Chiang et al. have revealed that edc4 binding to dcp1a is independent of its phosphorylation status while the phosphorylation status of dcp1a is important for its strong binding to dcp2 (decapping co-factor) (Chiang et al., 2013). Taken together, our data and these studies indicate that Ca^{2+} might have a role in mediating the interaction of dcp1a with other p-bodies and stress granule markers and the formation of mRNP granule composition through regulating phosphorylation. Therefore, further detailed studies are needed to elucidate the role of Ca^{2+} in the regulation of mRNP granule composition in undifferentiated and differentiated mESCs.

In our phosphoproteomic data, we have observed the upregulation of Atp5f1a, Cox4i1, Hk2, and downregulation of Pkm upon Ca^{2+} reduction which are important for oxidative

1) Institute for Stem Cell Science and Regenerative Medicine (inStem), Bangalore, India
2) Lead contact and corresponding author: shikha.ss19254@gmail.com

phosphorylation and mitochondrial fusion (Lis et al., 2016, Li et al., 2019, Čunátová et al., 2021). It has been already reported that undifferentiated ESCs have globular immature mitochondria and prefer glycolysis over oxidative phosphorylation whereas during differentiation mitochondria undergo conformation change and differentiated cells favour oxidative phosphorylation for energy production (Fu et al., 2019). Our data also suggest globular mitochondria in undifferentiated mESCs and long tubular mitochondria as well as an increase in the number of mitochondria upon Ca^{2+}reduction in mESCs which illustrate that low calcium might be needed for mitochondrial biogenesis and drive mitochondrial structural changes to support oxidative phosphorylation in differentiated mESCs. Taken together, our data indicate that calcium has a broad role in modulating various biological processes such as cell cycle arrest, protein stability, RNA splicing, mRNA stability, ribosome biogenesis, mRNP granule formation, ubiquitination, metabolism, telomere maintenance, oxidative phosphorylation, mitochondrial biogenesis, chromatin regulation, RNA polyadenylation for the maintenance of mESCs identity.

Experimental procedures

Resource availability: Further information and requests for reagents may be directed to and will be fulfilled by the lead contact: Shikha Sharma **(**shikha.ss19254@gmail.com**)**

Materials availability

This study did not generate new unique reagents.

Data and code availability

Affiliations:

1) Institute for Stem Cell Science and Regenerative Medicine (inStem), Bangalore, India
2) Lead contact and corresponding author: shikha.ss19254@gmail.com

Phosphoproteomics data is submitted to proteomeXchange consortrium MassIVE (https://massive.ucsd.edu/ProteoSAFe/static/massive.jsp). Dataset name: MSV000099451, Username: MSV000099451_reviewer , Password: A3THBj3Gj9pbMO1t

Culturing of mESCs and calcium modulation

mESCs E14TG2a and E14 cell lines were maintained on 0.1% gelatin at 37°C in a 5% CO2 incubator in ES medium containing high glucose DMEM (Gibco^{TM}), ESGRO recombinant mouse LIF, 15% ES cell FBS (Gibco^{TM}), β-Mercaptoethanol (Gibco^{TM}), 1x NEAA (Gibco^{TM}) and gentamycin (Gibco^{TM}). To induce spontaneous differentiation, mESCs were trypsinized with 0.05% Trypsin-EDTA (Gibco^{TM}) and cultured in ES media in the absence of LIF. For Bapta (Invitrogen^{TM}) and thapsigargin treatment, mESCS were cultured in the presence of LIF with different concentrations of bapta (1um and 2uM) and thapsigargin (250pm, 500pm and 1nM) for 72 hrs. Bapta and thapsigargin stock solutions were prepared using DMSO. An equal amount of DMSO was added into the control media as compared to bapta and thapsigargin. The medium was changed every day.

All other experimental procedures can be found in the supplementary file (S1)

Acknowledgements:

The work was supported by inStem core funds.

Author contributions

TM initiated the project. TM and SS have designed the experiments and performed the analysis. DP has given suggestions on p-body markers. SS performed all the experiments and wrote the manuscript with input from all authors.

Affiliations:

1) Institute for Stem Cell Science and Regenerative Medicine (inStem), Bangalore, India
2) Lead contact and corresponding author: shikha.ss19254@gmail.com

Declaration of interests

The authors declare no competing interests.

References

1. Bae, K.B., Yu, D.H., Lee, K.Y., Yao, K., Ryu, J., Lim, D.Y., Zykova, T.A., Kim, M.O., Bode, A.M., Dong, Z. Serine 347 Phosphorylation by JNKs Negatively Regulates OCT4 Protein Stability in Mouse Embryonic Stem Cells. Stem Cell Reports. 2017; 9: 2050-2064.
2. Ben-Nissan, G., Sharon, M. Regulating the 20S proteasome ubiquitin-independent degradation pathway. Biomolecules. 2014; 4: 862-84. doi: 10.3390/biom4030862.
3. Berridge, M.J., Bootman, M.D., Roderick, H.L. Calcium signalling: dynamics, homeostasis and remodelling. Nat Rev Mol Cell Biol. 2003; 4: 517-529.
4. Buchan, J.R. mRNP granules. Assembly, function, and connections with disease. RNA boil. 2014; 11: 1019-1030.
5. Chiang, P.Y., Shen, Y.F., Su, Y.L., Kao, C.H., Lin, N.Y., Hsu, P.H., Tsai, M.D., Wang, S.C., Chang, G.D., Lee, S.C., et al. Phosphorylation of mRNA decapping protein Dcp1a by the ERK signaling pathway during early differentiation of 3T3-L1 preadipocytes. PLoS One. 2013;8:e61697.
6. Clapham, D.E. (2007). Calcium signalling. Cell. 2007; 131: 1047-1058. doi: 10.1016/j.cell.2007.11.028.
7. Collatz, M.B., Rüdel, R., Brinkmeier, H. Intracellular calcium chelator BAPTA protects cells against toxic calcium overload but also alters physiological calcium responses. Cell Calcium. 1997;21:453-9.

Affiliations:

1) Institute for Stem Cell Science and Regenerative Medicine (inStem), Bangalore, India
2) Lead contact and corresponding author: shikha.ss19254@gmail.com

8. Čunátová, K., Reguera, D.P., Vrbacký, M., Fernández-Vizarra, E., Ding, S., Fearnley, IM., Zeviani, M., Houštěk, J., Mráček, T., Pecina, P. Loss of COX4I1 Leads to Combined Respiratory Chain Deficiency and Impaired Mitochondrial Protein Synthesis. Cells. 2021; 10(2): 369.
9. Czechanski, A., Byers, C., Greenstein, I., Schrode, N., Donahue, L.R., Hadjantonakis, A.K., Reinholdt, L.G. Derivation and characterization of mouse embryonic stem cells from permissive and nonpermissive strains. Nat Protoc. 2014; 9:559-74.
10. Decker, C.J., Parker, R. P-bodies and stress granules: possible roles in the control of translation and mRNA degradation. Cold Spring Harb Perspect Biol. 2012; 4(9): a012286.
11. Franchini, C., Fontana, F., Minuzzo, M., Babbio, F., Privitera, E. Apoptosis promoted by up-regulation of TFPT (TCF3 fusion partner) appears p53 independent, cell type restricted and cell density influenced. Apoptosis. 2006; 11: 2217-24.
12. Fu, W., Liu, Y., Yin, H. Mitochondrial Dynamics: Biogenesis, Fission, Fusion, and Mitophagy in the Regulation of Stem Cell Behaviors. Stem Cells Int. 2019; 2019: 9757201.
13. Hamazaki, T., Oka, M., Yamanaka, S., Terada, N. Aggregation of embryonic stem cells induces Nanog repression and primitive endoderm differentiation. J Cell Sci. 2004; 117: 5681–5686.
14. Han, Y.H., Moon, H.J., You, B.R., Park, W.H. The effect of MG132, a proteasome inhibitor on HeLa cells in relation to cell growth, reactive oxygen species and GSH. Oncol Rep. 2009; 22: 215-21. PMID: 19513526.

Affiliations:

1) Institute for Stem Cell Science and Regenerative Medicine (inStem), Bangalore, India
2) Lead contact and corresponding author: shikha.ss19254@gmail.com

15. Hochstoeger, T., Papasaikas, P., Piskadlo, E., Chao, J.A. Distinct roles of LARP1 and 4EBP1/2 in regulating translation and stability of 5'TOP mRNAs. Sci Adv. 2024; 10(7): eadi7830.
16. Hołubowicz, R., Wojtas, M., Taube, M., Kozak, M., Ożyhar, A., Dobryszycki, P. Effect of calcium ions on structure and stability of the C1q-like domain of otolin-1 from human and zebrafish. FEBS J. 2017; 284: 4278-4297. doi: 10.1111/febs.14308.
17. Kao, S.H., Wang, W.L., Chen, C.Y., Chang, Y.L., Wu, Y.Y., Wang, Y.T., Wang, S.P., Nesvizhskii, A.I., Chen, Y.J., Hong, T.M., et al.. Analysis of Protein Stability by the Cycloheximide Chase Assay. Bio Protoc. 2015; 5: e1374.
18. Kim, S.H, Kim, M.O., Cho, Y.Y., Yao, K., Kim, D.J., Jeong, C.H., Yu, D.H., Bae, K.B., Cho, E.J., Jung, S.K., et al. ERK1 phosphorylates Nanog to regulate protein stability and stem cell self-renewal. Stem Cell Res. 2014; 13: 1-11.
19. Kobayashi, H., Kikyo, N. Epigenetic regulation of open chromatin in pluripotent stem cells. Transl Res. 2015; 165: 18-27.
20. Liang, B., Zheng, W., Fang, L., Wu, L., Zhou, F., Yin, X., Yu, X., Zou, Z. Overexpressed targeting protein for Xklp2 (TPX2) serves as a promising prognostic marker and therapeutic target for gastric cancer. Cancer Biol Ther. 2016; 17: 824-32.
21. Li, T., Han, J., Jia, L., Hu, X., Chen, L., Wang, Y. PKM2 coordinates glycolysis with mitochondrial fusion and oxidative phosphorylation. Protein Cell. 2019; 10: 583-594.
22. Lis, P., Dyląg, M., Niedźwiecka, K., Ko, Y.H., Pedersen, P.L., Goffeau, A., Ułaszewski, S. The HK2 Dependent "Warburg Effect" and Mitochondrial Oxidative Phosphorylation in Cancer: Targets for Effective Therapy with 3-Bromopyruvate. Molecules. 2016; 21(12): 1730.

Affiliations:

1) Institute for Stem Cell Science and Regenerative Medicine (inStem), Bangalore, India
2) Lead contact and corresponding author: shikha.ss19254@gmail.com

23. Lytton, J., Westlin, M., Hanley, M.R. Thapsigargin inhibits the sarcoplasmic or endoplasmic reticulum Ca-ATPase family of calcium pumps. J Biol Chem. 1991; 266: 17067-71. PMID: 1832668.
24. Martinez, N.J., Chang, H.M., Borrajo, Jde. R., Gregory, R.I. The co-chaperones Fkbp4/5 control Argonaute2 expression and facilitate RISC assembly. RNA. 2013; 19(11): 1583-93. doi: 10.1261/rna.040790.113.
25. Mège, R.M., Ishiyama, N. Integration of Cadherin Adhesion and Cytoskeleton at Adherens Junctions. Cold Spring Harb Perspect Biol. 2017; 9(5): a028738. doi: 10.1101/cshperspect.a028738.
26. Niwa, H., Miyazaki, J., Smith, A.G. Quantative expression of OCT3/4 defines differentiation, dedifferentiation or self-renewal of ES cells. Nat Genetics. 2000; 24: 372176.
27. Ohtsuka. S., Nakai-Futatsugi, Y., Niwa, H. LIF signal in mouse embryonic stem cells. JAKSTAT. 2015; ;4(2): e1086520.
28. Olariu, V., Lovkvist, C., Sneppen, K.. (2016). Nanog, Oct4 and Tet1 interplay in establishing pluripotency. Sci Rep. 2016; 5: 25438.
29. Park, J.H., Chung, C.G., Park, S.S., Lee, D., Kim, K.M., Jeong, Y., Kim, E.S., Cho, J.H., Jeon, Y.M., Shen, C.J., et al. Cytosolic calcium regulates cytoplasmic accumulation of TDP-43 through Calpain-A and Importin α3. Elife. 2020; 9: e60132.
30. Pereverzev, A., Gurskaya, N., Ermakova, G,V., Kudryavtseva, E.I., Markina, N.M., Kotlobay, A.A., Lukyanov, S.A., Zaraisky, A.G., Lukyanov, K.A. Method for quantitative analysis of nonsense-mediated mRNA decay at the single cell level. Sci Rep. 2015; 5: 7729.

Affiliations:

1) Institute for Stem Cell Science and Regenerative Medicine (inStem), Bangalore, India
2) Lead contact and corresponding author: shikha.ss19254@gmail.com

31. Sanford, E.J., Smolka, M.B. Fe-NTA Microcolumn Purification of Phosphopeptides from Immunoprecipitation (IP) Eluates for Mass Spectrometry Analysis. Bio Protoc. 2021; 11(15): e4113.
32. Schwirtlich, M., Emri, Z., Antal, K., Mate, Z., Katarova, Z., Szabo, G. GABA(A) and GABA(B) receptors of distinct properties affect oppositely the proliferation of mouse embryonic stem cells through synergistic elevation of intracellular Ca(2+). FASEB J. 2010; 24: 1218–1228..
33. Strynadka, and James, 1991, Towards an understanding of the effects of calcium on protein structure and function. Current Opinion in Structural Biology. 1991; 1: 905-914.
34. Shang, F., Taylor, A. Ubiquitin-proteasome pathway and cellular responses to oxidative stress. Free Radic Biol Med. 2011; 51: 5-16.
35. Shim, J., Mukherjee, T., Mondal, B.C., Liu, T., Young, G.C., Wijewarnasuriya, D.P., Banerjee, U. Olfactory control of blood progenitor maintenance. Cell. 2013; 155:1141-53.
36. Sim, Y.J., Kim, M.S., Nayfeh, A., Yun, Y.J., Kim, S.J., Park, K.T., Kim, C.H., Kim, K.S. 2i Maintains a Naive Ground State in ESCs through Two Distinct Epigenetic Mechanisms. Stem Cell Reports. 2017; 8: 1312-1328.
37. Song, A., Ye, J., Zhang, K., Sun, L., Zhao, Y., Yu, H. Lentiviral vector-mediated siRNA knockdown of c-MYC: cell growth inhibition and cell cycle arrest at G2/M phase in Jijoye cells. Biochem Genet. 2013; 51: 603-17.
38. Tang, Y., Tian, X.C. JAK-STAT3 and somatic cell reprogramming. JAKSTAT. 2013 Oct 1;2(4):e24935.

Affiliations:

1) Institute for Stem Cell Science and Regenerative Medicine (inStem), Bangalore, India
2) Lead contact and corresponding author: shikha.ss19254@gmail.com

39. Tang, D., Chen, M., Huang, X., Zhang, G., Zeng, L., Zhang, G., Wu, S., Wang, Y. SRplot: A free online platform for data visualization and graphing. PLoS One. 2023; 18: e0294236. doi: 10.1371/journal.pone.0294236.
40. Todorova, M.G., Fuentes, E., Soria, B., Nadal, A., Quesada, I., Lysophosphatidic acid induces Ca2+ mobilization and c-Myc expression in mouse embryonic stem cells via the phospholipase C pathway. Cell. Signal. 2009; 21: 523–528.
41. Torres-Padilla, M.E., Chambers, I. Transcription factor heterogeneity in pluripotent stem cells: a stochastic advantage. Development. 2014; 141(11): 2173-81.
42. Wang, D., Xu, Q., Yuan, Q., Jia, M., Niu, H., Liu, X., Zhang, J., Young, C.Y., Yuan, H. Proteasome inhibition boosts autophagic degradation of ubiquitinated-AGR2 and enhances the antitumor efficiency of bevacizumab. Oncogene. 2019; 38: 3458–3474.
43. Xu, H., Van Remmen, H. The SarcoEndoplasmic Reticulum Calcium ATPase (SERCA) pump: a potential target for intervention in aging and skeletal muscle pathologies. Skeletal Muscle. 2021; 11:25.
44. Yanagida, E., Shoji, S., Hirayama, Y., Yoshikawa, F., Otsu, K., Uematsu, H., Hiraoka, M.,Furuichi, T., Kawano, S. . Functional expression of Ca2+ signalingpathwaysin mouse embryonic stem cells. Cell Calcium. 2004; 36: 135–146.
45. Yeo, J.C and Ng, H.H. (2013). The transcriptional regulation of pluripotency. Cell Res. 2013; 23: 20-32.
46. Ying, Q-L., Wray, J., Nichols, J., Batlle-Morera, L., Doble, B., Woodgett ,J., Cohen, P., Smith, A. The ground state of embryonic stem cell self-renewal. Nature. 2008; 453:519-23.
47. Ye, Y., Xie, W., Ma, Z. Wang, X., Wen, Y., Li, X., Qi, H., Wu, H., An, J., Jiang, Y., et al. Conserved mechanisms of self-renewal and pluripotency in mouse and human

Affiliations:

1) Institute for Stem Cell Science and Regenerative Medicine (inStem), Bangalore, India
2) Lead contact and corresponding author: shikha.ss19254@gmail.com

ESCs regulated by simulated microgravity using a 3D clinostat. Cell Death Discov. 2024;. 10:68 (2024).

Figure Legends

Figure 1: Calcium level in mESCs: A) Fluo4 staining, B) DIER reporter expression, C) Fluo4 and lysotracker staining of mESCs under different conditions (C+L, B2uM, T1nM, C-L, C-L+T1nM) (n=3-5).

D and E) Bar plot represents the mean intensity of fluo4 staining and ER gcamp in mESCs calculated from the confocal images of the above experiments.

F) Bar graph showing the percentage of the proliferation of mESCs treated with B1uM, B2uM, and B5uM for 72 hrs compared to control using the trypan blue method (n=4).

G) Bar graph showing percentage of the proliferation of mESCs treated with B2uM and B5uM for 5 days and B2R condition compared to control D2 and D5 respectively (n=4)

H) Western blot detection of cMyc in the presence and absence of B2uM for 72hrs (n=2)

I) Immunofluorescence (IF) detection of cMyc expression in mESCs in the presence of B2uM for 5 days and B2R condition (n=3)

J) The bar plot represents the mean intensity of cMyc expression calculated from the confocal images of the above experiments.

K) QPCR of cMyc expression in mESCs treated with B2uM for 72hrs (n=3).

L) Cell cycle analysis of control (D2) and B2uM treated mESCs for 72 hrs (n=4). Significant p-value (0.0085) was detected for B2/D2 (G2/M)

M) Cell cycle analysis of D2, B2uM treated mESCs for 5 days and B2R condition (n=5). Significant p-value (0.0003 and 0.01) was detected for B2/D2 and B2R/B2 (G2/M)

Affiliations:

1) Institute for Stem Cell Science and Regenerative Medicine (inStem), Bangalore, India
2) Lead contact and corresponding author: shikha.ss19254@gmail.com

C+L= Control + Lif; B1uM= Control + Lif + Bapta 1uM; B2uM = Control + Lif + Bapta 2uM; T250 pm, T500pm, and T nM= Control + thapsigargin (250 pm, 500pm, and 1nM), C-L= control without Lif, D2= C+L+ dmso equivalent to B2uM condition

The mean intensity was calculated from the confocal images for all experiments using ImageJ software. P-value representation with asterisk <0.05 (*), <0.01 (**), <0.001 (***), <0.0001 (****).

Figure 2: Role of calcium in pluripotency: IF detection of **A)** Nanog (red), **B)** Oct4 (green), **C)** pCamkIIα (red), **D)** Oct4, pCamkIIα and Dapi co-staining in mESCs cultured under different conditions (C+L, B2uM, T1nM, C-L, C-L+T1nM) (n=3)

E) Western blot shows the expression of Oct4, Nanog, pSTAT3 and Gapdh in mESCs cultured under different conditions (C+L, B1uM, B2uM, C-L) (n=3).

F) Western blot shows the expression of Oct4, Nanog, pSTAT3 and Gapdh in mESCs cultured under different condition (C+L+T250pm, C+L+T500pm, C+L+T1nM) (n=3)

G) Western blot showed expression of Nanog in mESCs cultured under different conditions (C-L, C-L+T250pm, C-L+T500pm, C-L+T1nM)

H) Western blot showed expression of pSTAT3 and cMyC in mESCs cultured under different conditions (C-L, C-L+T1nM)

I, J) QPCR of pluripotency markers and early differentiation markers under different conditions (C+L, B2uM, T1nM, C-L, C-L+T1nM) (n=5)

K) Brightfield images of the mESCs cultured under different conditions (C+L, B2uM, T1nM, C-L, C-L+T1nM) (n=5)

L) IF detection of Phalloidin in mESCs cultured under different conditions as above (n=3)

M) The bar graph represents the mean intensity of Oct4, Nanog and pCamkII**α** expression calculated from the confocal images of the above experiments (A, B, C).

N) IF detection of E-cadherin staining in mESCs cultured under different conditions (C+L, B2uM, T1nM, C-L)

Affiliations:

1) Institute for Stem Cell Science and Regenerative Medicine (inStem), Bangalore, India
2) Lead contact and corresponding author: shikha.ss19254@gmail.com

Figure 3: Role of calcium at post-transcriptional level: A) IF detection of dcp1a, β-actin, xrn1a, pCamkIIα, tudor in mESCs cultured under different conditions (C+L, B2uM, T1nM, C-L) (n=3-5) using confocal microscopy at 60x magnification.

B) Co-localization expression profile of dcp1a and β-actin**;** dcp1a and xrn1**;** dcp1a and pCamkIIα**;** dcp1a and tudor in mESCs cultured under different condition (C+L, B2uM, T1nM, C-L, C-L+T1nM). To observe granule size and co-localization of p-bodies and stress granule markers, the images obtained using a confocal microscope at 60x magnification were cropped to one nucleus size and normalized using a 5uM marker at the bottom.

C) QPCR of p-bodies and stress granule markers (dcp1a, xrn1, **t**udor and pCamkIIα) in the mESCs cultured in the presence of B2uM for 72hrs.

D) The bar graph represents the mean intensity of dcp1a, xrn1, pCamkIIα and **t**udor expression calculated from confocal images from the above experiments (A).

E) IF detection of splicing dependent NMD by using NMD+ GFP, NMD+RFP, NMD-GFP, NMD-RFP reporter in mESCs cultured under different conditions (C+L, B2uM, C-L) (n=3).

F) Splicing-dependent NMD activity was calculated from the confocal images of the above experiments described by Pereverzev et al. 2015.

G) IF detection of long 3' UTR dependent NMD by using SMG+ GFP, SMG+RFP, pTRAM-GFP, pTRAM-RFP reporter in mESCs cultured under different conditions (C+L, B2uM, C-L) (n=3).

H) 3' UTR-dependent NMD activity was calculated from the confocal images of the above experiments as described by Pereverzev et al. 2015.

Figure 4: **Role of calcium at translational level: A)** Polysome profile of C+L and B2uM treated mESCs. (n=5)

Affiliations:

1) Institute for Stem Cell Science and Regenerative Medicine (inStem), Bangalore, India
2) Lead contact and corresponding author: shikha.ss19254@gmail.com

B) IF detection of Elf1a expression in mESCs cultured under different conditions (C+L, B2uM, C-L) using confocal microscopy at 60x magnification. (n=3)

C) The bar graph represents the mean intensity of Elf1a expression calculated from the confocal images of the above experiments.

D, E) QPCR of core proliferation and early differentiation markers in the cytoplasmic, 80s, polysome fraction of polysome profiling of control (D2) and B2uM treated mESCs. (n=4)

F, G) QPCR of core proliferation markers and early differentiation markers of mESCS cultured under different conditions (C+L, B2uM, C-**L, C-L+Tti)** for 72hrs followed by combined CHX and ACD treatment (TTi) for 2hr. (n=5)

H) IF detection of brachyury and Nanog expression in mESCs cultured under different conditions (C+L, B2uM, C-L). (n=3)

I) Confocal detection of mitochondria using mitotracker-red staining in mESCs cultured under different conditions (C+L, B2uM, C-L) for 48 hours using confocal microscopy at 40x magnification. To observe the mitochondria shape, images were cropped to one nucleus and normalized using a 5uM marker at the bottom. (n=4)

J) Confocal detection of mitochondria and calcium level using mitotracker-red and fluo-4 co-staining in mESCs cultured under condition (C+L and B2uM) (n=3).

Figure 5: Role of calcium at post-translational level: IF detection of **A)** Brachyury, and cMyc, **B)** dcp1a, and Tudor, **C)** Oct4 and pUBQ expression mESCs cultured under different conditions (D2, B2uM and C-L) for 72hrs followed by MG132 (10uM) treatment for 1 hr (n=3).

The bar plot represents the mean intensity of the expression profile of **D)** Brachyury, **E)** cMyc, **F)** dcp1a, and Tudor, **G)** Oct4 and pUBQ from the confocal images of the above experiments.

H) Western blot detection of autophagy marker LC3 in mESCs cultured under different conditions (C+L, B2uM, C-L). (n=3)

Affiliations:

1) Institute for Stem Cell Science and Regenerative Medicine (inStem), Bangalore, India
2) Lead contact and corresponding author: shikha.ss19254@gmail.com

I) Cycloheximide chase assay was performed for oct4 and Nanog protein in mESCs cultured under D2, B2uM conditions for 72hrs followed by addition of CHX (50 ug/ml) and chased for every 20min for 1 hr 20 min using western blotting. (n=3)

J) Oct4 and Nanog expression was detected by western blot in mESCs cultured under D2, B2uM conditions for 72hrs followed by the addition of MG132 (10uM) for 1hr. (n=3)

Note: D2= C+L+dmso equivalent to B2M condition; D2_MG = D2+MG132; B2uM= C+L+ Bapta 2uM; B2_MG = B2uM+MG132

Figure 6: knockdown of pCamkIIα in mESCsA) Detection of GFP expression of pCamkIIα shRNA and SERCA shRNA transfected by electroporation method in mESCs using fluorescent microscopy at 10X.

Brightfield images showing the morphology of the **B)** control mESCs, **C)** pCamkIIα shRNA (pCamkIIα KD) and SERCA shRNA (SER_R2_KD) transfected mESCs at 48hrs.

D) QPCR of pCamkIIα and serca R2 receptor expression in the mESCs at 48hrs upon pCamkIIα KD and SER_R2_ KD respectively

E) QPCR of pCamkIIα expression in the SER_R2 KD mESCs and serca_R2 receptor expression in the pCamkIIα KD mESCs at 48hrs.

F, G) Western blot detection of Oct4, Nanog, pSTAT3, and Gapdh expression in the pCamkIIα KD and SER_R2_KD mESCs at 48hrs (n=3)

H, I) IF detection of DCP1a and pCamkIIα co-expression in pCamkIIα and SER_R2 KD mESCs at 48hrs. (n=3)

J, K) Bar plot represents the mean intensity of pCamkIIα and dcp1a expression in mESCs calculated from the confocal images of the above experiments

L) QPCR of p-bodies and stress granule markers in the mESCs at 48hrs upon pCamkIIα KD and ser_R2 KD. (n=4)

Affiliations:

1) Institute for Stem Cell Science and Regenerative Medicine (inStem), Bangalore, India
2) Lead contact and corresponding author: shikha.ss19254@gmail.com

M, N) QPCR of pluripotency and differentiation markers in the mESCs at 48hrs upon pCamkIIα KD and SER_R2 KD. (n=3)

Figure 7: Calcium and phosphoproteomics in mESCs: A) Heat map shows log2fold change of DEPP in B2uM treated mESCs compared to D2 (control) mESCs detected by mass spectrometry (n=2)

B, C, E) KEGG pathway and GOC enrichment analysis was done using ShinyGO 0.80 software for the DEPP represented in the heat map (A).

D) The hierarchical clustering tree shows the correlation among the most significant pathways found in KEGG pathway enrichment analysis for all DEPP.

F) The bar plot shows the string enrichment function analysis of all the DEPP demonstrated in the heat map.

G, H) KEGG pathway enrichment analysis was done for spliceosome and mRNA surveillance pathways all the DEPP represented in heat map (A).

I) String PPI network analysis was performed for all DEPP represented in a heat map (A).

Note: Arrow represent the upregulated and downregulated genes

Affiliations:

1) Institute for Stem Cell Science and Regenerative Medicine (inStem), Bangalore, India
2) Lead contact and corresponding author: shikha.ss19254@gmail.com

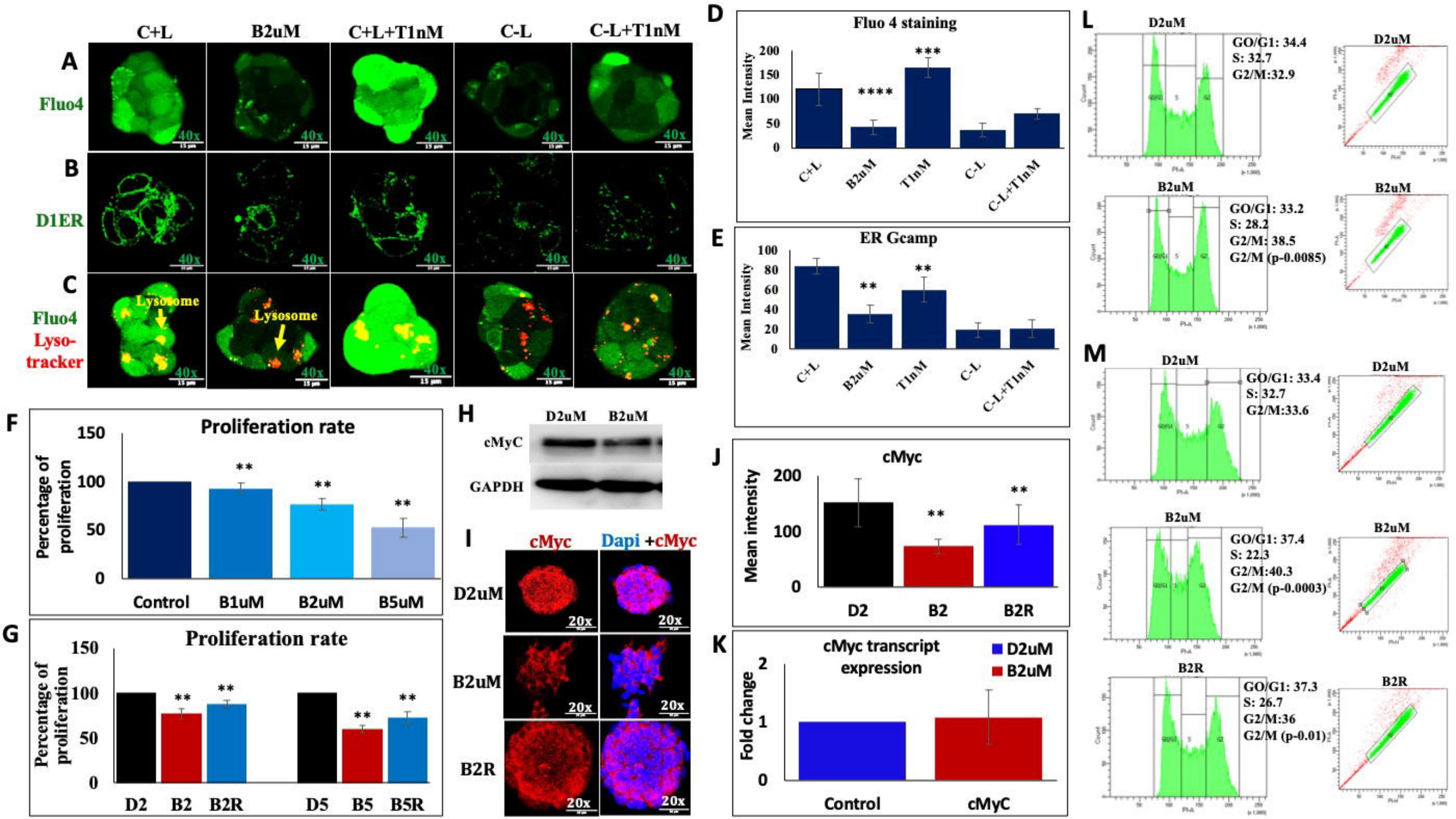
C+L
B2uM
C+L+T1nM
C-L
C-L+T1nM
A
Fluo4
B
D1ER
C
Fluo4
Lyso-tracker
Lysosome
40x
D
Fluo 4 staining
Mean Intensity
200
150
100
50
0
****
***
C+L
B2uM
T1nM
C-L
C-L+T1nM
E
ER Gcamp
Mean Intensity
100
80
60
40
20
0
**
**
C+L
B2uM
T1nM
C-L
C-L+T1nM
F
Proliferation rate
Percentage of proliferation
150
100
50
0
**
**
**
Control
B1uM
B2uM
B5uM
G
Proliferation rate
Percentage of proliferation
150
100
50
0
**
**
**
**
D2
B2
B2R
D5
B5
B5R
H
D2uM
B2uM
cMyC
GAPDH
I
cMyc
Dapi +cMyc
D2uM
B2uM
B2R
20x
J
cMyc
Mean intensity
200
100
0
**
**
D2
B2
B2R
K
cMyc transcript expression
D2uM
B2uM
Fold change
2
1
0
Control
cMyC
L
D2uM
GO/G1: 34.4
S: 32.7
G2/M:32.9
B2uM
GO/G1: 33.2
S: 28.2
G2/M: 38.5
G2/M (p-0.0085)
M
D2uM
GO/G1: 33.4
S: 32.7
G2/M:33.6
B2uM
GO/G1: 37.4
S: 22.3
G2/M:40.3
G2/M (p-0.0003)
B2R
GO/G1: 37.3
S: 26.7
G2/M:36
G2/M (p-0.01)

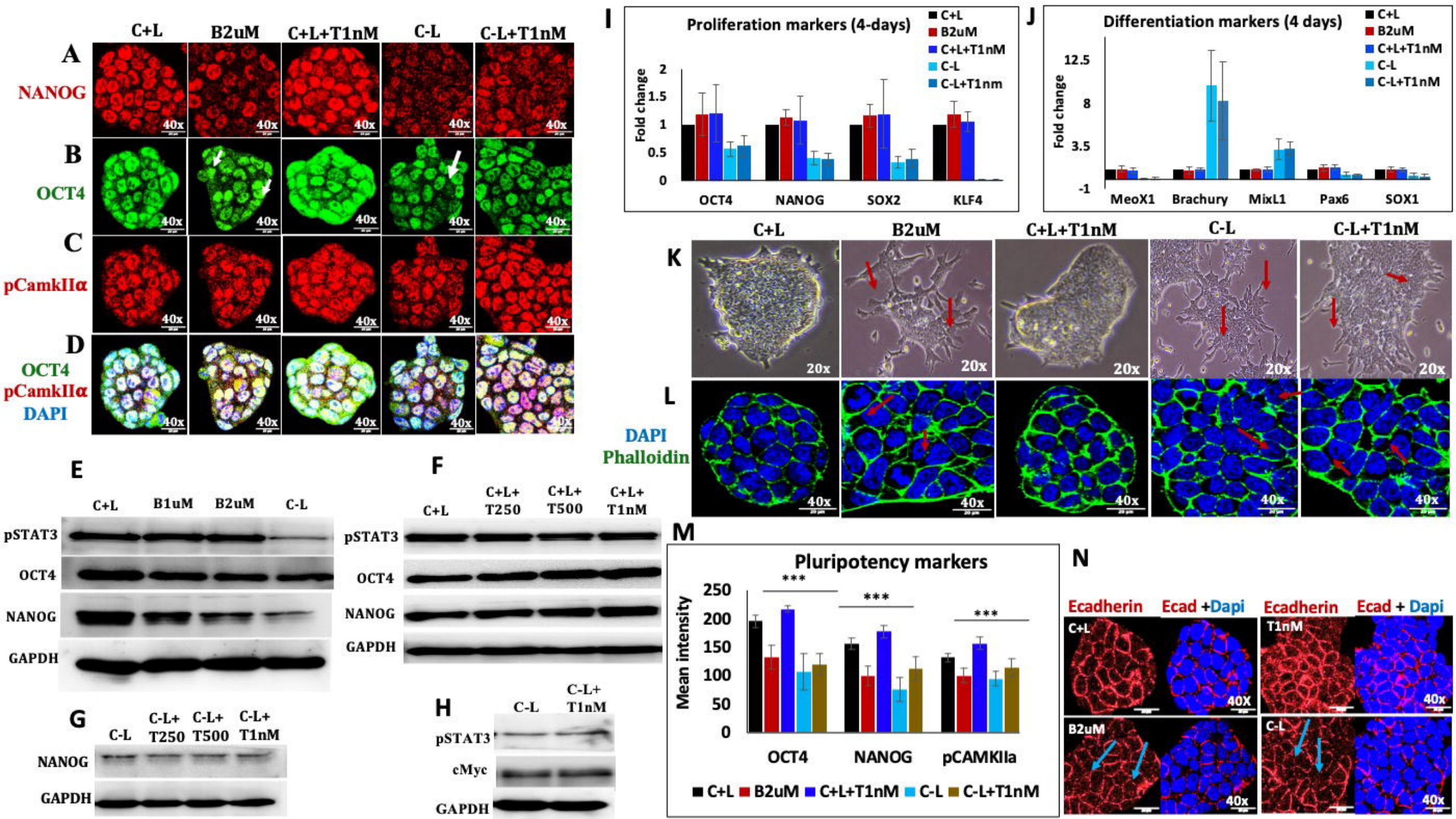
A
C+L
B2uM
C+L+T1nM
C-L
C-L+T1nM
NANOG
B
OCT4
C
pCamkIIα
D
OCT4
pCamkIIα
DAPI
40x
I
Proliferation markers (4-days)
C+L
B2uM
C+L+T1nM
C-L
C-L+T1nm
Fold change
OCT4
NANOG
SOX2
KLF4
J
Differentiation markers (4 days)
Fold change
MeoX1
Brachury
MixL1
Pax6
SOX1
K
20x
L
DAPI
Phalloidin
E
C+L
B1uM
B2uM
C-L
pSTAT3
OCT4
NANOG
GAPDH
F
C+L
C+L+ T250
C+L+ T500
C+L+ T1nM
G
C-L
C-L+ T250
C-L+ T500
C-L+ T1nM
H
cMyc
M
Pluripotency markers
Mean intensity
***
pCAMKIIa
N
Ecadherin
Ecad +Dapi
Ecad + Dapi
T1nM

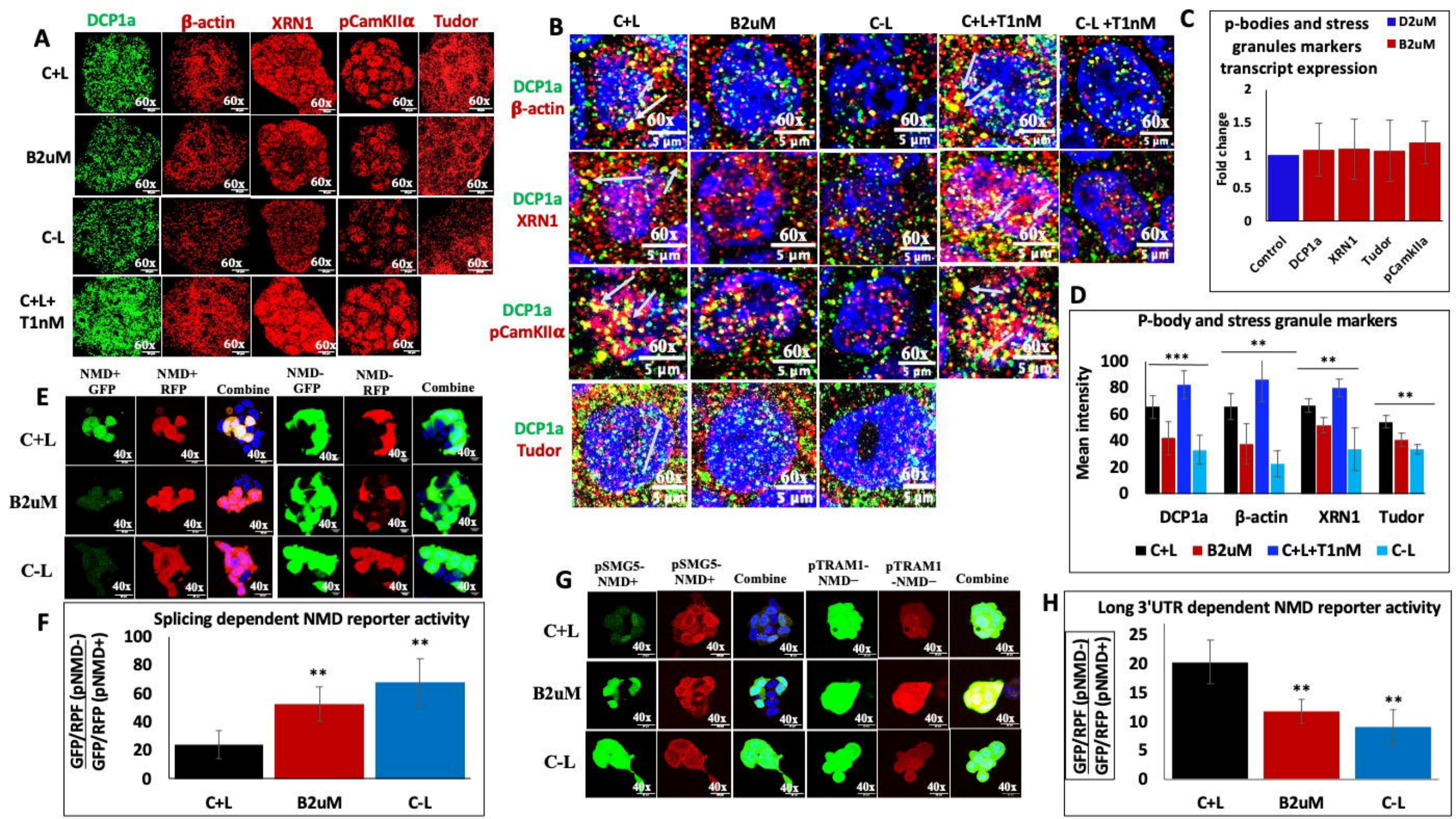
A
DCP1a
β-actin
XRN1
pCamKIIα
Tudor
C+L
B2uM
C-L
C+L+ T1nM
60x
B
C+L
B2uM
C-L
C+L+T1nM
C-L +T1nM
DCP1a β-actin
DCP1a XRN1
DCP1a pCamKIIα
DCP1a Tudor
5 µm
C
p-bodies and stress granules markers transcript expression
D2uM
B2uM
Fold change
Control
DCP1a
XRN1
Tudor
pCamkIIa
D
P-body and stress granule markers
Mean intensity
DCP1a
β-actin
XRN1
Tudor
C+L
B2uM
C+L+T1nM
C-L
E
NMD+ GFP
NMD+ RFP
Combine
NMD- GFP
NMD- RFP
Combine
C+L
B2uM
C-L
40x
F
Splicing dependent NMD reporter activity
GFP/RPF (pNMD-)
GFP/RFP (pNMD+)
C+L
B2uM
C-L
G
pSMG5-NMD+
pSMG5-NMD+
Combine
pTRAM1-NMD−
pTRAM1 -NMD−
Combine
C+L
B2uM
C-L
H
Long 3'UTR dependent NMD reporter activity
GFP/RPF (pNMD-)
GFP/RFP (pNMD+)
C+L
B2uM
C-L

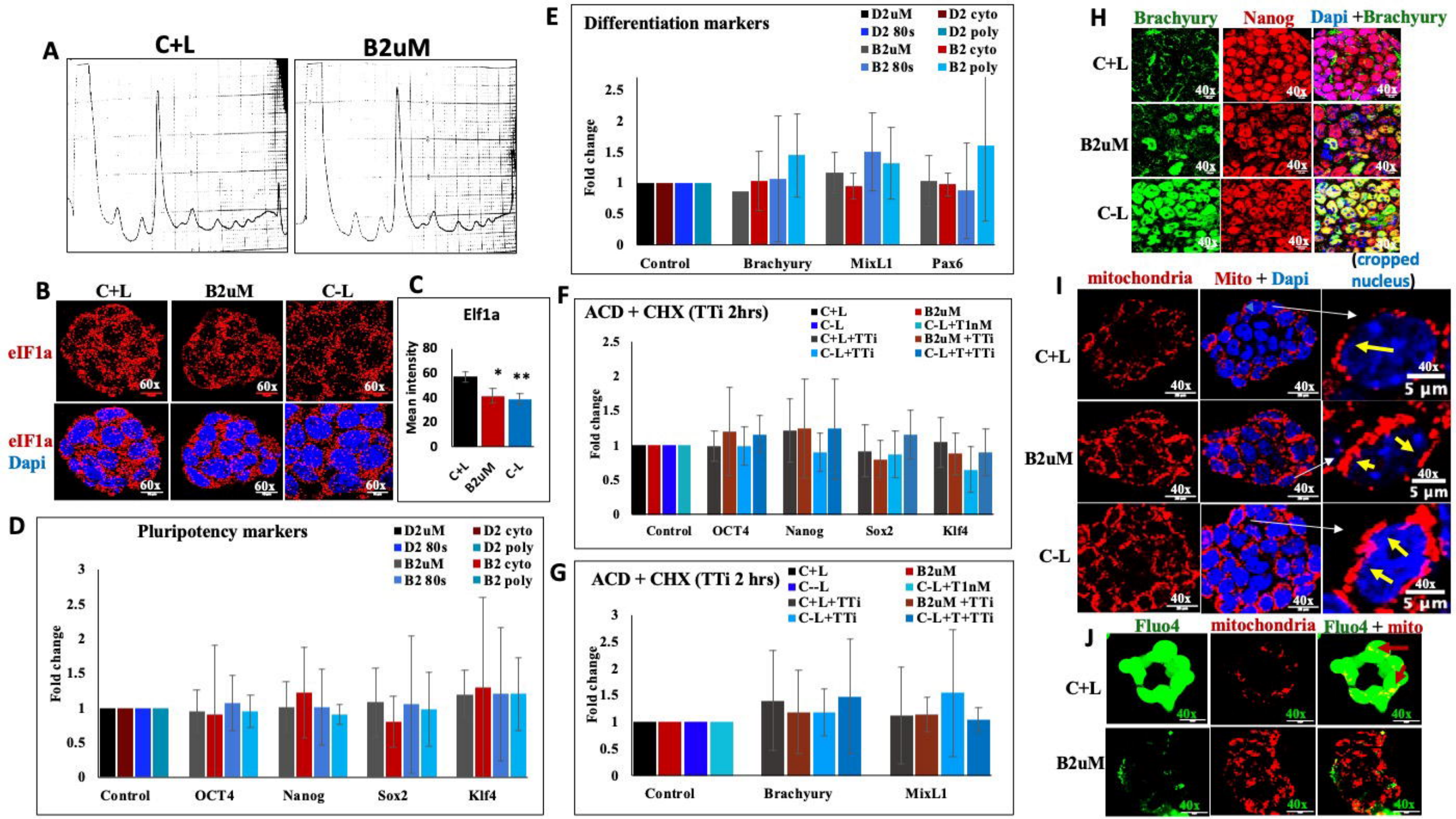
A
C+L
B2uM
B
C+L
B2uM
C-L
eIF1a
eIF1a
Dapi
60x
C
Elf1a
Mean intensity
80
60
40
20
0
*
**
C+L
B2uM
C-L
D
Pluripotency markers
D2uM
D2 cyto
D2 80s
D2 poly
B2uM
B2 cyto
B2 80s
B2 poly
Fold change
3
2.5
2
1.5
1
0.5
0
Control
OCT4
Nanog
Sox2
Klf4
E
Differentiation markers
D2uM
D2 cyto
D2 80s
D2 poly
B2uM
B2 cyto
B2 80s
B2 poly
Fold change
2.5
2
1.5
1
0.5
0
Control
Brachyury
MixL1
Pax6
F
ACD + CHX (TTi 2hrs)
C+L
B2uM
C-L
C-L+T1nM
C+L+TTi
B2uM +TTi
C-L+TTi
C-L+T+TTi
Fold change
2.5
2
1.5
1
0.5
0
Control
OCT4
Nanog
Sox2
Klf4
G
ACD + CHX (TTi 2 hrs)
C+L
B2uM
C--L
C-L+T1nM
C+L+TTi
B2uM +TTi
C-L+TTi
C-L+T+TTi
Fold change
3
2.5
2
1.5
1
0.5
0
Control
Brachyury
MixL1
H
Brachyury
Nanog
Dapi +Brachyury
C+L
B2uM
C-L
40x
I
mitochondria
Mito + Dapi
(cropped nucleus)
C+L
B2uM
C-L
40x
5 µm
J
Fluo4
mitochondria
Fluo4 + mito
C+L
B2uM
40x

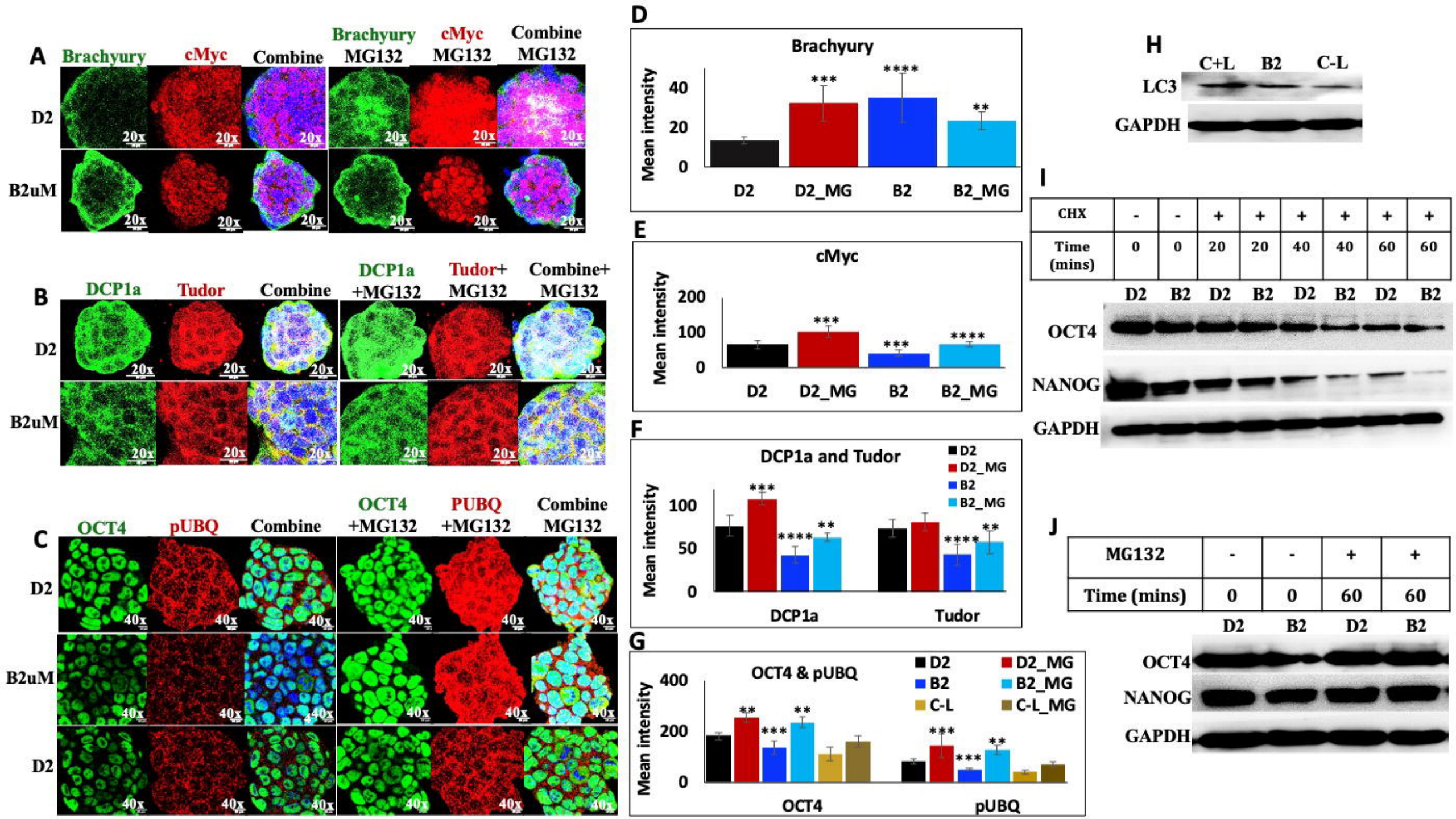
A
Brachyury
cMyc
Combine
Brachyury MG132
cMyc MG132
Combine MG132
D2
B2uM
20x
B
DCP1a
Tudor
Combine
DCP1a +MG132
Tudor+ MG132
Combine+ MG132
C
OCT4
pUBQ
Combine
OCT4 +MG132
PUBQ +MG132
Combine MG132
40x
D
Brachyury
Mean intensity
D2
D2_MG
B2
B2_MG
E
cMyc
F
DCP1a and Tudor
DCP1a
Tudor
G
OCT4 & pUBQ
OCT4
pUBQ
C-L
C-L_MG
H
C+L
LC3
GAPDH
I
CHX
Time (mins)
OCT4
NANOG
J
MG132

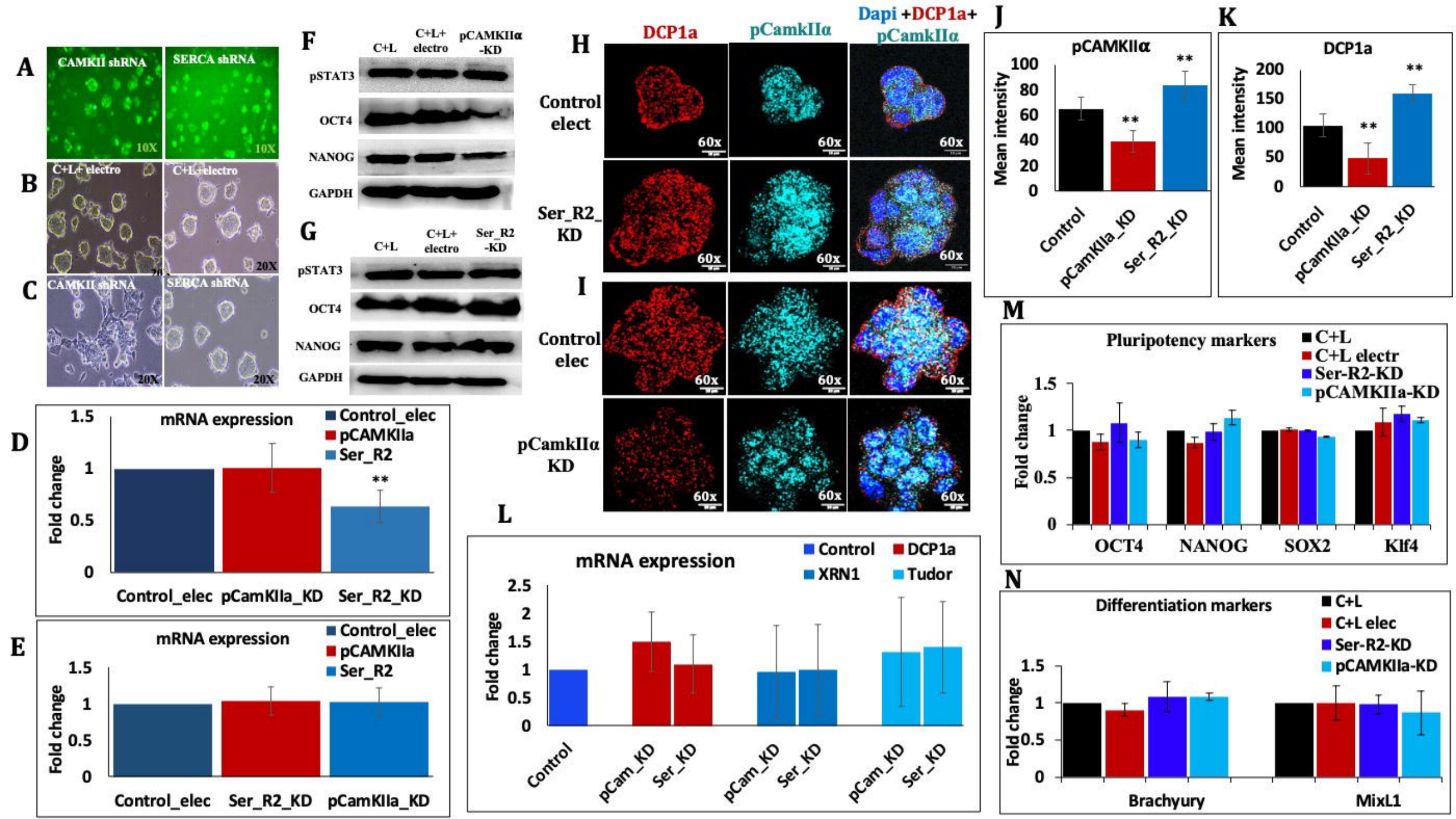
A
CAMKII shRNA
SERCA shRNA
10X
10X
B
C+L+ electro
C+L+electro
20X
20X
C
CAMKII shRNA
SERCA shRNA
20X
20X
F
C+L
C+L+ electro
pCAMKIIα -KD
pSTAT3
OCT4
NANOG
GAPDH
G
C+L
C+L+ electro
Ser_R2 -KD
pSTAT3
OCT4
NANOG
GAPDH
H
DCP1a
pCamkIIα
Dapi +DCP1a+ pCamkIIα
Control elect
Ser_R2_ KD
60x
I
Control elec
pCamkIIα KD
60x
J
pCAMKIIα
Mean intensity
100
80
60
40
20
0
**
**
Control
pCamKIIa_KD
Ser_R2_KD
K
DCP1a
Mean intensity
200
150
100
50
0
**
**
Control
pCamKIIa_KD
Ser_R2_KD
M
Pluripotency markers
C+L
C+L electr
Ser-R2-KD
pCAMKIIa-KD
Fold change
1.5
1
0.5
0
OCT4
NANOG
SOX2
Klf4
D
mRNA expression
Control_elec
pCAMKIIa
Ser_R2
Fold change
1.5
1
0.5
0
**
Control_elec
pCamKIIa_KD
Ser_R2_KD
E
mRNA expression
Control_elec
pCAMKIIa
Ser_R2
Fold change
1.5
1
0.5
0
Control_elec
Ser_R2_KD
pCamKIIa_KD
L
mRNA expression
Control
DCP1a
XRN1
Tudor
Fold change
2.5
2
1.5
1
0.5
0
Control
pCam_KD
Ser_KD
pCam_KD
Ser_KD
pCam_KD
Ser_KD
N
Differentiation markers
C+L
C+L elec
Ser-R2-KD
pCAMKIIa-KD
Fold change
1.5
1
0.5
0
Brachyury
MixL1

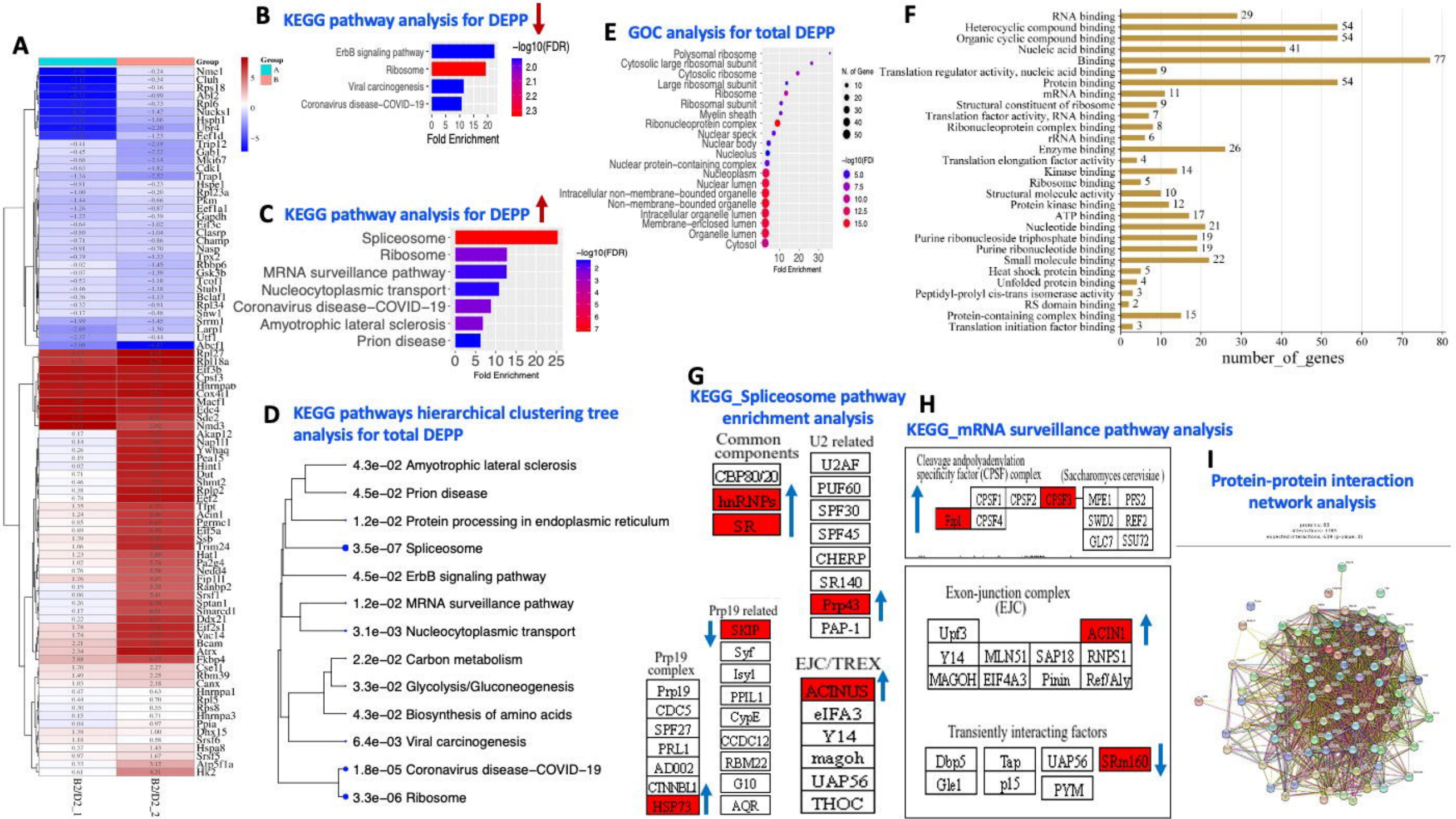
A
Group
Nmc1
Cluh
Rps18
Abl2
Rpl6
Nucks1
Hsph1
Ubr4
Eef1d
Trip12
Gab1
Mki67
Cdk1
Trap1
Hspe1
Rpl23a
Pkm
Eef1a1
Gapdh
Eif3c
Clasrp
Champ
Nasp
Tpx2
Rbbp6
Gsk3b
Tcof1
Stub1
Bclaf1
Rpl34
Snw1
Srrm1
Larp1
Utf1
Abcf1
Rpl27
Rpl18a
Eif3b
Cpsf3
Hnrnpab
Cox4i1
Macf1
Edc4
Sde2
Nmd3
Akap12
Nap1l1
Ywhaq
Pea15
Hint1
Dut
Shmt2
Rplp2
Eef2
Tipt
Acin1
Pgrmc1
Eif5a
Ssb
Trim24
Hat1
Pa2g4
Nedd4
Fip1l1
Ranbp2
Srsf1
Sptan1
Smarcd1
Ddx21
Eif2s1
Vac14
Bcam
Atrx
Fkbp4
Cse1l
Rbm39
Canx
Hnrnpa1
Rpl5
Rps8
Hnrnpa3
Ppia
Dhx15
Srsf6
Hspa8
Srsf5
Atp5f1a
HK2
B2/D2_1
B2/D2_2
B
KEGG pathway analysis for DEPP
ErbB signaling pathway
Ribosome
Viral carcinogenesis
Coronavirus disease-COVID-19
Fold Enrichment
-log10(FDR)
C
KEGG pathway analysis for DEPP
Spliceosome
Ribosome
MRNA surveillance pathway
Nucleocytoplasmic transport
Coronavirus disease-COVID-19
Amyotrophic lateral sclerosis
Prion disease
Fold Enrichment
-log10(FDR)
D
KEGG pathways hierarchical clustering tree analysis for total DEPP
4.3e-02 Amyotrophic lateral sclerosis
4.5e-02 Prion disease
1.2e-02 Protein processing in endoplasmic reticulum
3.5e-07 Spliceosome
4.5e-02 ErbB signaling pathway
1.2e-02 MRNA surveillance pathway
3.1e-03 Nucleocytoplasmic transport
2.2e-02 Carbon metabolism
3.3e-02 Glycolysis/Gluconeogenesis
4.3e-02 Biosynthesis of amino acids
6.4e-03 Viral carcinogenesis
1.8e-05 Coronavirus disease-COVID-19
3.3e-06 Ribosome
E
GOC analysis for total DEPP
Polysomal ribosome
Cytosolic large ribosomal subunit
Cytosolic ribosome
Large ribosomal subunit
Ribosome
Ribosomal subunit
Myelin sheath
Ribonucleoprotein complex
Nuclear speck
Nuclear body
Nucleolus
Nuclear protein-containing complex
Nucleoplasm
Nuclear lumen
Intracellular non-membrane-bounded organelle
Non-membrane-bounded organelle
Intracellular organelle lumen
Membrane-enclosed lumen
Organelle lumen
Cytosol
Fold Enrichment
N. of Gene
-log10(FDR)
F
RNA binding
Heterocyclic compound binding
Organic cyclic compound binding
Nucleic acid binding
Binding
Translation regulator activity, nucleic acid binding
Protein binding
mRNA binding
Structural constituent of ribosome
Translation factor activity, RNA binding
Ribonucleoprotein complex binding
rRNA binding
Enzyme binding
Translation elongation factor activity
Kinase binding
Ribosome binding
Structural molecule activity
Protein kinase binding
ATP binding
Nucleotide binding
Purine ribonucleoside triphosphate binding
Purine ribonucleotide binding
Small molecule binding
Heat shock protein binding
Unfolded protein binding
Peptidyl-prolyl cis-trans isomerase activity
RS domain binding
Protein-containing complex binding
Translation initiation factor binding
number_of_genes
G
KEGG_Spliceosome pathway enrichment analysis
Common components
CBP80/20
hnRNPs
SR
U2 related
U2AF
PUF60
SPF30
SPF45
CHERP
SR140
Prp43
PAP-1
Prp19 related
SKIP
Syf
Isy1
PPIL1
CypE
CCDC12
RBM22
G10
AQR
Prp19 complex
Prp19
CDC5
SPF27
PRL1
AD002
CTNNBL1
HSP73
EJC/TREX
ACINUS
eIFA3
Y14
magoh
UAP56
THOC
H
KEGG_mRNA surveillance pathway analysis
Cleavage andpolyadenylation specificity factor (CPSF) complex
(Saccharomyces cerevisiae)
CPSF1
CPSF2
CPSF3
Fip1
CPSF4
MPE1
PFS2
SWD2
REF2
GLC7
SSU72
Exon-junction complex (EJC)
Upf3
ACIN1
Y14
MLN51
SAP18
RNPS1
MAGOH
EIF4A3
Pinin
Ref/Aly
Transiently interacting factors
Dbp5
Tap
UAP56
SRm160
Gle1
p15
PYM
I
Protein-protein interaction network analysis